

Exponentiated Weibull model for the irradiance probability density function of a laser beam propagating through atmospheric turbulence

Ricardo Barrios*, Federico Dios

Department of Signal Theory and Communications, Universitat Politècnica de Catalunya, C/ Jordi Girona 1-3, Campus Nord, D-3, 08034 Barcelona, Spain

ARTICLE INFO

Article history:

Received 15 June 2012

Received in revised form

18 July 2012

Accepted 2 August 2012

Available online 27 August 2012

Keywords:

Exponentiated Weibull

Atmospheric turbulence

Channel model

ABSTRACT

Many distributions have been proposed to model the probability density function of irradiance fluctuations. The most widespread models nowadays are the Lognormal (LN) and Gamma–Gamma (GG) distributions. Albeit these models comply with the actual PDF data most of the time, neither of them works in all scenarios and, depending on the conditions, one of the two have to be chosen. In this paper, a new model is presented resulting in the exponentiated Weibull (EW) distribution, along with a physical justification for the appearance of the model. Previously published data are used to compare the new model with the LN and GG distributions. Results suggest that the EW distribution is the better fit for data under all aperture averaging conditions and weak-to-strong turbulence regime.

© 2012 Elsevier Ltd. All rights reserved.

1. Introduction

For many decades the scientific community, dedicated to the study of the atmospheric turbulence effects in free-space optical (FSO) communication links, have been in the search for a probability density function (PDF) capable to model the fluctuations of the signal-carrying laser beam intensity. Many distribution have been proposed over the years, all with different degrees of success. Historically, the models that drawn more attention were the lognormally modulated Rician distribution – also known as the Beckmann distribution – [1], the lognormally modulated exponential distribution [2], and the *I*–*K* distribution introduced by Andrews and Phillips [3] as a generalization of the well-known *K*-distribution [4]. But, nowadays, the two most widely accepted models are the Lognormal (LN) and Gamma–Gamma (GG) distributions [5].

The major difficulty continues to be finding a unique distribution to model the PDF of the irradiance fluctuations, valid in all regimes of turbulence strength and under all aperture averaging conditions. Many authors report that the LN model is valid in weak turbulence regime for a point receiver and works well in all regimes of turbulence when a fair amount of aperture averaging occurs [6,7]. For strong turbulence the LN model was also accepted until additional work [8,9] showed that this assumption is not valid under certain conditions [10]. On the other hand, the GG model is accepted to be valid in all turbulence regimes for a

point receiver, nevertheless, the GG model does not hold when aperture averaging takes place [5,6,10].

In this paper a new model is presented resulting in the exponentiated Weibull (EW) distribution, first proposed by Barrios and Dios to model the distribution of the irradiance in FSO links, and tested under weak turbulence regime for numerical simulation and experimental data [11]. The EW distribution was introduced by Mudholkar and Srivastava [12] as a generalization of the well-known Weibull distribution, with the addition of an extra shape parameter. The Weibull distribution – initially appearing in the field of reliability engineering – have been extensively used in physics and engineering, to model the wind speed distribution [13], particle size distribution [14], a specific type of clutter [15], and, in wireless communications where some channels are modeled with Weibull fading [16,17].

Additionally, previously published data are used to explore the exponentiated Weibull model suitability compared with the Lognormal and Gamma–Gamma distributions.

The next section offers a brief summary on the LN and GG distribution. Section 3 is devoted to present a physical justification for the new model. Section 4 focuses on comparing the LN, GG, and EW distributions using data from both numerical simulations and experimental data. Finally, Section 4.3 is devoted to discuss the results of the comparison and conclusions are extracted.

2. Background

A laser beam propagating through the atmosphere will be altered by refractive-index inhomogeneities. At the receiver

* Corresponding author. Tel.: +34 934017426; fax: +34 934017232.

E-mail addresses: ricardo.barrios@tsc.upc.edu (R. Barrios), fede@tsc.upc.edu (F. Dios).

plane, a random pattern is produced both in time and space [18]. The parameter for describing the fluctuations of the received optical power I is the scintillation index (SI), and it is defined by

$$\sigma_I^2 = \frac{\langle I^2 \rangle}{\langle I \rangle^2} - 1, \quad (1)$$

where the brackets $\langle \cdot \rangle$ denote an ensemble average. Therefore, the SI is directly related to the normalized second-order moment of the irradiance, which can be derived from the probability density function governing the random variable I .

Taking the fact that the scintillation index can be estimated from atmospheric parameters [19] and using Eq. (1), the defining parameters of the irradiance PDF can be, thus, predicted from atmospheric parameters. Note that it is customary to normalize the irradiance data in the sense that $\langle I \rangle = 1$.

Next the PDF of the two most accepted models is presented, namely the Lognormal and Gamma–Gamma distribution. The cumulative distribution functions (CDF) are presented for completeness.

2.1. Lognormal distribution

The PDF and CDF of a random variable I described by the Lognormal (LN) distribution are given by

$$f_{\text{LN}}(I; \sigma_{\ln I}^2) = \frac{1}{I\sqrt{2\pi\sigma_{\ln I}^2}} \exp\left\{-\frac{[\ln(I) + 0.5\sigma_{\ln I}^2]^2}{2\sigma_{\ln I}^2}\right\} \quad (2)$$

and

$$F_{\text{LN}}(I; \sigma_{\ln I}^2) = \frac{1}{2} + \frac{1}{2} \operatorname{erf}\left[\frac{\ln(I) + 0.5\sigma_{\ln I}^2}{\sqrt{2\sigma_{\ln I}^2}}\right], \quad (3)$$

respectively; where $\sigma_{\ln I}^2$ is the variance of the log-irradiance, and it is related to the scintillation index by

$$\sigma_{\ln I}^2 = \ln(\sigma_I^2 + 1). \quad (4)$$

2.2. Gamma–Gamma distribution

The PDF of a random variable I described by the Gamma–Gamma (GG) distribution is given by

$$f_{\text{GG}}(I; \alpha, \beta) = \frac{2(\alpha\beta)^{(\alpha+\beta)/2}}{\Gamma(\alpha)\Gamma(\beta)} I^{(\alpha+\beta)/2-1} K_{\alpha-\beta}(2\sqrt{\alpha\beta I}), \quad (5)$$

where $K_\nu(x)$ is the modified Bessel function of the second kind of order ν , and, α and β are parameters directly related to the scintillation index by

$$\sigma_I^2 = \frac{1}{\alpha} + \frac{1}{\beta} + \frac{1}{\alpha\beta}. \quad (6)$$

The Gamma–Gamma distribution is used to model the two independent contributions of the small-scale and large-scale atmospheric effects, assuming that each of them is governed by a Gamma process. Therefore, the parameters of the GG model can be related to the small-scale scintillation index $\sigma_Y^2 = 1/\beta$ and large-scale scintillation index $\sigma_X^2 = 1/\alpha$ [5].

The cumulative distribution function of the GG model is not shown here as it has a long complex form, and it is rather cumbersome to evaluate numerically. The expression of the CDF can be found in Al-Habash et al. [5].

3. New model

3.1. Weibull fading

Let us first assume a very simple fading model. An optical wave propagating in the turbulent atmosphere can be regarded as a circular complex Gaussian random field $U = X_1 + jX_2 = X \exp(-j\varphi)$, where $j^2 = -1$ [20]. Considering that X_1 and X_2 are zero-mean Gaussian processes with variance σ^2 , then, the random phase $\varphi = \tan^{-1}(X_2/X_1)$ is uniformly distributed in $[0, 2\pi)$, and the amplitude of the optical wave $X = \sqrt{X_1^2 + X_2^2}$ is Rayleigh distributed, with probability density function

$$f_R(x; \Omega) = \frac{2x}{\Omega} \exp\left(-\frac{x^2}{\Omega}\right), \quad (7)$$

where $\Omega = E[x^2]$ is a scale parameter; and $E[\cdot]$ denotes the expected value. Now let the received irradiance to be obtained from a nonlinear function of the squared modulus of the wave's amplitude X . Such a nonlinearity is manifested in terms of a power parameter $\beta > 0$, so that the received signal intensity is the result of not simply the squared modulus of X , but this squared modulus to a certain power [21]. Therefore, the received random signal is $Y = U^{2/\beta} = X^{2/\beta} \exp(-j2\varphi/\beta)$, and the corresponding PDF of the irradiance $I = X^{2/\beta}$ follows a Weibull distribution defined as

$$f_W(I; \beta, \eta) = \frac{\beta}{\eta} \left(\frac{I}{\eta}\right)^{\beta-1} \exp\left[-\left(\frac{I}{\eta}\right)^\beta\right], \quad (8)$$

where $\beta > 0$ is a shape parameter, and $\eta > 0$ is a scale parameter, that depends on β , and is related to the mean value of the irradiance. For the special cases of $\beta = 2$ and $\beta = 1$, Eq. (8) reduces to the Rayleigh and negative exponential PDF, respectively.

The cumulative distribution function (CDF) of a random variable I having the Weibull distribution is defined by

$$F_W(I; \beta, \eta) = 1 - \exp\left[-\left(\frac{I}{\eta}\right)^\beta\right]. \quad (9)$$

It is easily proved that the n -th irradiance moment of the Weibull PDF is given by

$$\langle I^n \rangle = \eta^n \Gamma\left(1 + \frac{n}{\beta}\right), \quad (10)$$

where the brackets $\langle \cdot \rangle$ denote expectation, and $\Gamma(\cdot)$ is the gamma function.

Combining Eqs. (1) and (10), the scintillation index is given by [22, Eq. (6–15)]

$$\sigma_I^2 = \frac{\Gamma(1+2/\beta)}{\Gamma(1+1/\beta)^2} - 1 \approx \beta^{-11/6}, \quad (11)$$

a good approximation for $\beta \geq 1$.

For the derivation of the scale parameter η , without loss of generality, the irradiance data is normalized in the sense that $\langle I \rangle = 1$, and setting $n=1$ in Eq. (10), yields

$$\eta = \frac{1}{\Gamma(1+1/\beta)}. \quad (12)$$

3.2. Exponentiated Weibull fading

Models in which the fading is characterized by a single PDF are only valid for stationary conditions, where the statistics of the channel are somehow invariant over the observation time period. On the other hand, if the process of interest is nonstationary and the signal statistics vary significantly over the interval of interest, a mixture of model is better suited, where a weighted summation of several statistical distributions can be used [23].

Let us now, extend the simple Weibull fading channel model. Assume an optical wave propagating in the turbulent atmosphere, with multiple scatterers and random refractive-index variations. As the wave travels through this medium, multipath scattering components start to appear and cause irradiance random fluctuations of the signal-carrying laser beam. Indeed, if the coherence radius of the initial beam is significantly smaller than the beam radius, the process of propagation of the laser beam can be considered as the independent propagation of a large number of coherent beams [24]. Then, the observed field at the receiver is, thus, composed by a on-axis component and a weak multipath term, composed by scattered components via different independent off-axis paths. The physical reason for this partition of the received optical field is supported by the high directivity inherent to laser beams sources. This propagation model is very similar to that proposed by Jurado-Navas et al. [25], but here the term coupled with the on-axis component is dropped.

Considering the above physical justification, the observed field irradiance I is assumed to be a weighted summation of several mutually independent irradiance random variables. Taking into account that a simple summation is only valid for noncoherent beams, and that the degree of coherence of such waves and even the number of separable or independent components is unknown a generalized average is used, in order to provide the necessary degree of freedom to the mathematical model to account for the partially coherent regime, as follows

$$I^p = \sum_{i=1}^m w_i I_i^p, \quad (13)$$

where I_i are Weibull random variables, and w_i are weighting factors accounting for the mean attenuation of each path. This factors are normalized such that $\sum w_i = 1$. The on-axis component is denoted by I_1 , and there are $m-1$ off-axis terms. Moreover, instead of a summation of linear components it is assumed the existence of a nonlinear relationship—as in the Weibull fading model—manifested in terms of a power parameter $p > 0$.

Now, supported by the fact that the on-axis term is on average greater than the multipath component one can try to make an approximation of the summation in Eq. (13). The naive alternative would be to drop all the off-axis, but this would lead to the simple Weibull fading model derived above. Then, in order to approximate such summation to the on-axis component, but still considering the off-axis terms the maximum function can be introduced as

$$I = \lim_{p \rightarrow \infty} \left[\sum_{i=1}^m w_i I_i^p \right]^{1/p} = \max\{I_1, I_2, \dots, I_m\}, \quad (14)$$

where I_1, I_2, \dots, I_m are independent and identically distributed Weibull random variables of the irradiance data. Therefore, the cumulative distribution function of I_i is given by Eq. (9), and using the property of ordered statistics for the maximum of a sample the CDF of the irradiance is $F(I) = [F_W(I)]^m$ [26, Eq. (5.3b)]. These types of distributions are referred in the literature as exponentiated distributions, where m is a nonnegative integer number.

Furthermore, it is a natural assumption to define $\alpha > 0$ as the real valued extension of m . This allows for a less stringent model, where noninteger values may account for nonzero correlation among the components of different propagation paths [21]. Therefore, the parameter α can be interpreted as the average number of on-axis plus off-axis components effectively intervening in a given observation period.

Physical intuition tells us that the α parameter should be low for weak turbulence, as there are few scatterers lowering the probability of off-axis components to appear, increasing to a maximum value somewhere in the moderate turbulence regime,

as the number of scatterers increases too. Nevertheless, when approaching the strong turbulence regime this value should decrease as—although there are a higher number of scatterers in the optical path—the off-axis components easily deviate in such a way that the probability of missing the receiver increases. Moreover, the value of α can be lower than unity denoting deep fading events where, during the observation time period, on average even the on-axis component could not reach the receiver.

Then, the PDF and CDF of a random variable I described by the exponentiated Weibull (EW) distribution are given by

$$f_{EW}(I; \alpha, \beta, \eta) = \frac{\alpha\beta}{\eta} \left(\frac{I}{\eta}\right)^{\beta-1} \exp\left[-\left(\frac{I}{\eta}\right)^\beta\right] \times \left\{1 - \exp\left[-\left(\frac{I}{\eta}\right)^\beta\right]\right\}^{\alpha-1} \quad (15)$$

and

$$F_{EW}(I; \alpha, \beta, \eta) = \left\{1 - \exp\left[-\left(\frac{I}{\eta}\right)^\beta\right]\right\}^\alpha, \quad (16)$$

respectively; where $\beta > 0$ and $\alpha > 0$ are shape parameters related to the SI, and $\eta > 0$ is a scale parameter, and it is related to the mean value of the irradiance. It is noteworthy that for $\alpha = 1$ Eq. (15) reduces to the Weibull distribution—i.e. Eq. (8).

The n -th irradiance moment of the exponentiated Weibull PDF has recently been derived for any α , both real and integer, and has the form [27]

$$\langle I^n \rangle = \alpha \eta^n \Gamma\left(1 + \frac{n}{\beta}\right) g_n(\alpha, \beta), \quad (17)$$

where $g_n(\alpha, \beta)$ was introduced to simplify the notation, and is defined by

$$g_n(\alpha, \beta) = \sum_{i=0}^{\infty} \frac{(-1)^i \Gamma(\alpha)}{i!(i+1)^{1+n/\beta} \Gamma(\alpha-i)}. \quad (18)$$

Eq. (18) is easily computed numerically as the series converges rapidly, and usually as much as 10 terms or less are sufficient for the series to converge.

Combining Eq. (1) and (17), the EW parameters can be related with the scintillation index as

$$\sigma_I^2 = \frac{\Gamma(1+2/\beta) g_2(\alpha, \beta)}{\alpha [\Gamma(1+1/\beta) g_1(\alpha, \beta)]^2} - 1. \quad (19)$$

As it is readily seen from Eq. (17), the analytical derivation of the EW parameters is rather a complex task. Therefore, a heuristic approach was used to obtain a relation between the EW parameters and the scintillation index. Thus, using the simulation data from Barrios and Dios [11], the shape parameter β was found to be related with the scintillation index and the parameter α as

$$\beta \simeq 1.012(\alpha \sigma_I^2)^{-13/25} + 0.142. \quad (20)$$

This expression is a mere refinement of the previous proposal [11].

Then, this relation was used to graphically solve Eq. (19), as the numeric methods tried resulted in unstable solutions. In this manner, a set of data point relating the shape parameter α and the SI were plotted. Next, using standard curve fitting techniques the parameter α was found to approximately follow

$$\alpha \simeq \frac{7.220 \sigma_I^{2/3}}{\Gamma(2.487 \sigma_I^{2/6} - 0.104)}. \quad (21)$$

This is a completely new expression compared with the initial proposal in Barrios and Dios [11], which was found to work only in some particular cases. The expression given here has a wider applicability.

Finally, the scale parameter η is given by

$$\eta = \frac{1}{\alpha \Gamma(1 + 1/\beta) g_1(\alpha, \beta)}. \quad (22)$$

4. Comparison with published data

In this section already published data are used to assess the Gamma–Gamma and Lognormal model fit to the probability density function of the irradiance, as the two most widely accepted models nowadays. Moreover, a comparison of these models to the proposed exponentiated Weibull PDF is made.

For completeness of this study numerical simulation results as well as experimental data are used. The simulation data were extracted from Vetelino et al. [28], while the experimental data used can be found in Wayne et al. [29]. Note that, in some figures, the original axes limits are changed aiming for a better resolution allowing straight forward comparison of the different PDF curves plotted.

The parameter values for each distribution are presented in Tables 1 and 2. For the sake of clarity some parameters have the subscript ‘fit’ or ‘data’, meaning that their values are extracted directly from the fitting process or the data itself. If no subscript is found, then, the value of such parameter was estimated with the corresponding expression of those given above.

4.1. Simulation data

The numerical simulation data presented in Vetelino et al. [28] were intended to reproduce the experimental results of a testbed where a 1550 nm continuous-wave laser, with 0.46 mrad full-angle divergence, was used. The beam was launched in a 1500 m horizontal path and, at the receiver plane, the optical power was detected using three simultaneous photodetectors of 1, 5, and 13 mm with no collecting lenses. For the simulation the smallest aperture used is 1.8 mm instead of 1 mm [28].

Table 1
Parameters for the LN, GG and EW distributions used to generate PDF curves in Fig. 1. The general conditions of the simulations, and the estimated scintillation index for the GG and EW distributions are also shown.

Aperture	Conditions			LN	GG			Exponentiated Weibull			
D (mm)	σ_{ldata}^2	σ_{R}^2	A	$\sigma_{\text{ln } I}^2$	α_{fit}	β_{fit}	$\hat{\sigma}_{\text{fit}}^2$	α	β	η	$\hat{\sigma}_I^2$
1.8	1.23	2.70	1.00	0.80	1.49	3.00	1.23	5.93	0.50	0.14	1.23
1.8	3.55	19.20	1.00	1.51	0.88	0.88	3.56	5.57	0.36	0.05	3.55
5.0	1.19	2.70	0.98	0.78	1.83	2.42	1.19	5.92	0.51	0.14	1.19
5.0	3.15	19.20	0.98	1.42	0.96	0.96	3.17	5.66	0.37	0.06	3.15
13.0	1.01	2.70	0.93	0.70	2.38	2.38	1.02	5.88	0.55	0.17	1.01
13.0	2.16	19.20	0.93	1.15	1.28	1.28	2.17	5.87	0.41	0.08	2.15

Table 2
Parameters for the LN, GG and EW distributions used to generate PDF curves in Fig. 2. The general conditions of the experiments, and the estimated scintillation index for the GG and EW distributions are also shown.

Aperture	Conditions			LN		GG		Exponentiated Weibull			
D (mm)	σ_{data}^2	σ_R^2	A	σ_{LN}^2	α_{fit}	β_{fit}	σ_{fit}^2	α	β	η	σ_I^2
4.0	4.57	10.30	0.96	2.00	1.30	1.30	2.13	5.33	0.34	0.04	4.57
4.0	2.25	2.50	0.96	1.78	1.60	1.60	1.64	5.85	0.41	0.08	2.24
20.6	1.50	11.10	0.62	1.16	2.10	2.10	1.18	5.94	0.47	0.11	1.50
20.6	0.84	2.10	0.62	0.73	3.00	3.00	0.78	5.81	0.59	0.19	0.84
154.0	0.14	7.00	0.03	0.15	7.60	95.50	0.14	4.19	1.49	0.62	0.14
154.0	0.05	1.90	0.03	0.06	34.50	34.50	0.06	3.04	2.86	0.84	0.05

Simulation was conducted with an optics wave code based on the spectral method of the split-step technique, in which phase screens are generated in the spectral domain by means of filtering Gaussian white noise with the second-order statistics of the selected turbulence power spectrum [30–32]. The power spectrum chosen is the Kolmogorov’s spectrum, therefore the inner and outer scales of turbulence are ignored. In this case the turbulence strength C_n^2 used corresponds to the value inferred from the experimental data.

The probability density function of the irradiance fluctuations is generated from 40,000 realizations for each case, and then plotted as a function of the normalized log irradiance. It should be noted that the PDF values for the GG and LN distributions are obtained by the transformation [28]

$$f_X(z) = f_X(l) \left| \frac{dl}{dz} \right|_{l=e^z} = e^z f_X(e^z), \quad (23)$$

where $f_X(\cdot)$ is given by either Eq. (2) or Eq. (5), and $z = \ln l$ is the natural logarithm of the normalized irradiance.

The simulation data PDFs shown in Fig. 1 correspond to those presented in Fig. 3 of Vetelino et al. [28]. Furthermore, in Table 1 all the defining parameters of the three PDFs being studied are listed, along with the receiving aperture size, scintillation index, Rytov variance $\sigma_R^2 = 1.23 C_n^2 k^{7/6} L^{11/6}$ and the aperture averaging factor A given by [33]

$$A = \left[1 + 0.333 \left(\frac{kD^2}{4L} \right)^{5/6} \right]^{-7/5}, \quad (24)$$

where $k = 2\pi/\lambda$ is the wavenumber, being λ the optical wavelength; D is the receiving aperture diameter, and L is the distance between the transmitter and receiver planes.

Note that the scintillation index σ_{data}^2 was calculated directly from the simulation data, and the σ_{LN}^2 parameter in the LN model was obtained from Eq. (4). The α_{fit} and β_{fit} parameters, presented in Table 1, are those found by a fitting process in Vetelino et al. [28], and the σ_{fit}^2 was calculated using Eq. (6), for the GG distribution.

On the other hand the α , β and η parameters, in the proposed EW model, were obtained from the equations presented in Section 3.2, are also listed in Table 1. These parameters along with Eq. (19) are used to calculate the scintillation index σ_I^2 for the EW distribution. Additionally, all the plots in Fig. 1 include the best fit of the exponentiated Weibull distribution to the PDF data and the estimated parameter values are embedded in each plot, as well as the scintillation index determined from such parameters. The Levenberg–Marquardt least-square algorithm was used to get the best fit estimation of the EW parameters [34,35].

4.2. Experimental data

The data presented in Wayne et al. [29] correspond to an experimental setup, consisting in continuous-wave 532 nm solid-state laser (4 mrad full-angle divergence) followed by a defocused

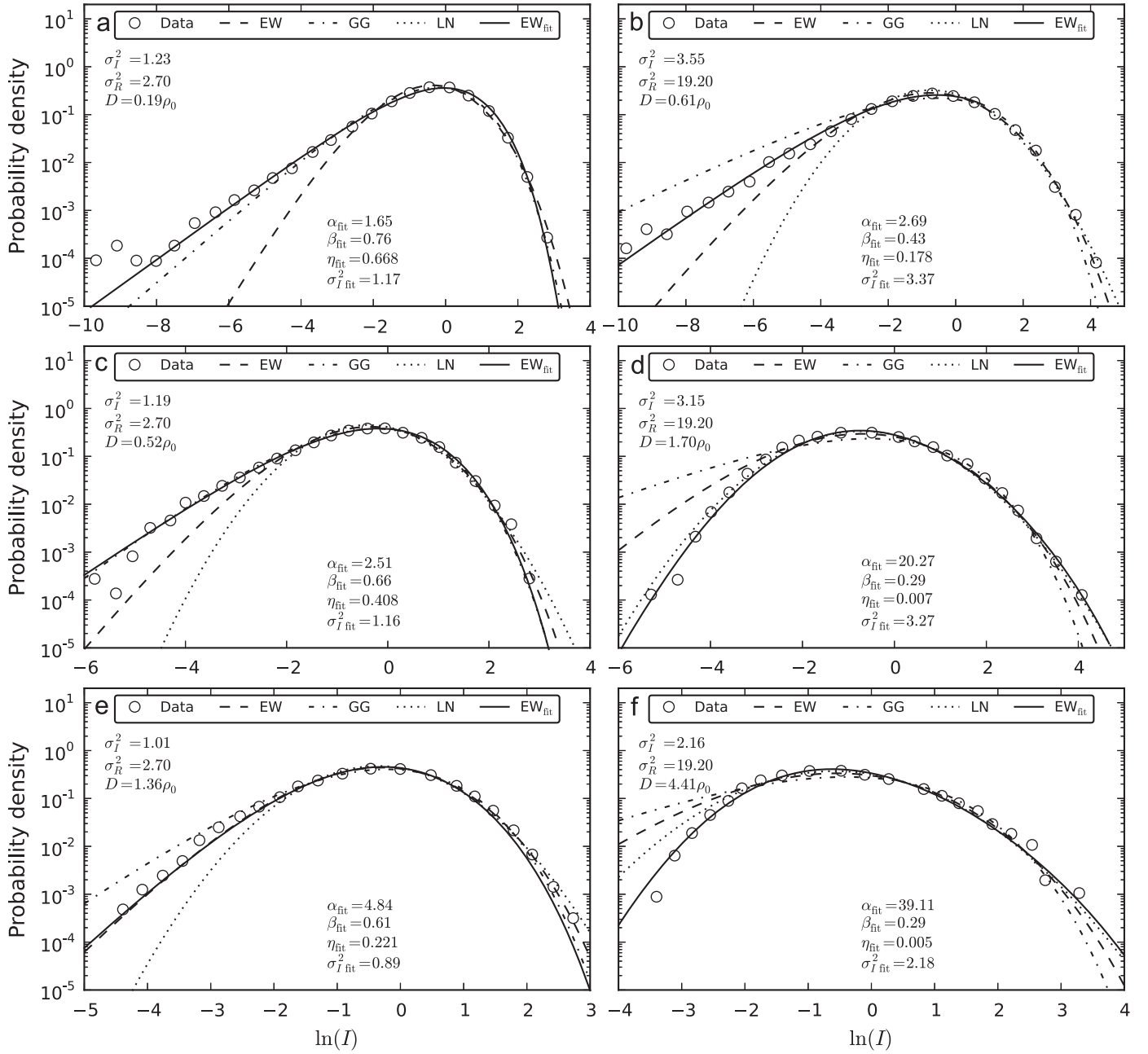


Fig. 1. Simulation data PDF from Vetelino et al. [28] in comparison with the EW distribution. The curves are plotted using the parameters from Table 1. The best fit curve for the EW distribution (solid line) is shown along with its parameters values.

beam expander, which produces an approximately spherical wave. The laser was launched in 1 km long testbed, and the receiver telescope was a 6 in (1 in=2.54 cm) diameter refracting lens. All the data were collected in 2 min runs by means of a 24 bits digitizer operating at 51.25 kS/s, producing a total of 6.15×10^6 samples to construct the experimental PDF for each run. The probability density function was generated by sorting the data using unequal bin widths, thus, avoiding the appearance of zero-count bins in the PDF.

The PDFs plots in Fig. 2 correspond to the receiving aperture diameters 4, 20.6 and 154 mm from Figs. 3 and 4 in Wayne et al. [29]. In Table 2 all the defining parameters of the three PDFs being studied are listed. For the experimental data case the $\sigma_{\ln I}^2$ parameter in the LN model as well as the α and β parameters in the GG model were determined by doing a best fit of the PDF data. The rest of the parameters in Table 2 were filled following the

same approach as in Table 1. Again, all the plots in Fig. 2 include the best fit of the exponentiated Weibull distribution to the PDF data.

4.3. Discussion

In this section, the Lognormal and the Gamma–Gamma distributions have been compared to a new proposed model, namely the exponentiated Weibull distribution. In order to conduct this study already published data have been used, corresponding to numerical simulations [28] and experiments [29]. In both scenarios the respective authors reach to the same conclusion, neither distribution—i.e. the LN and GG models—can model the probability density function of the irradiance fluctuations under all aperture averaging conditions and every atmospheric turbulence regime.

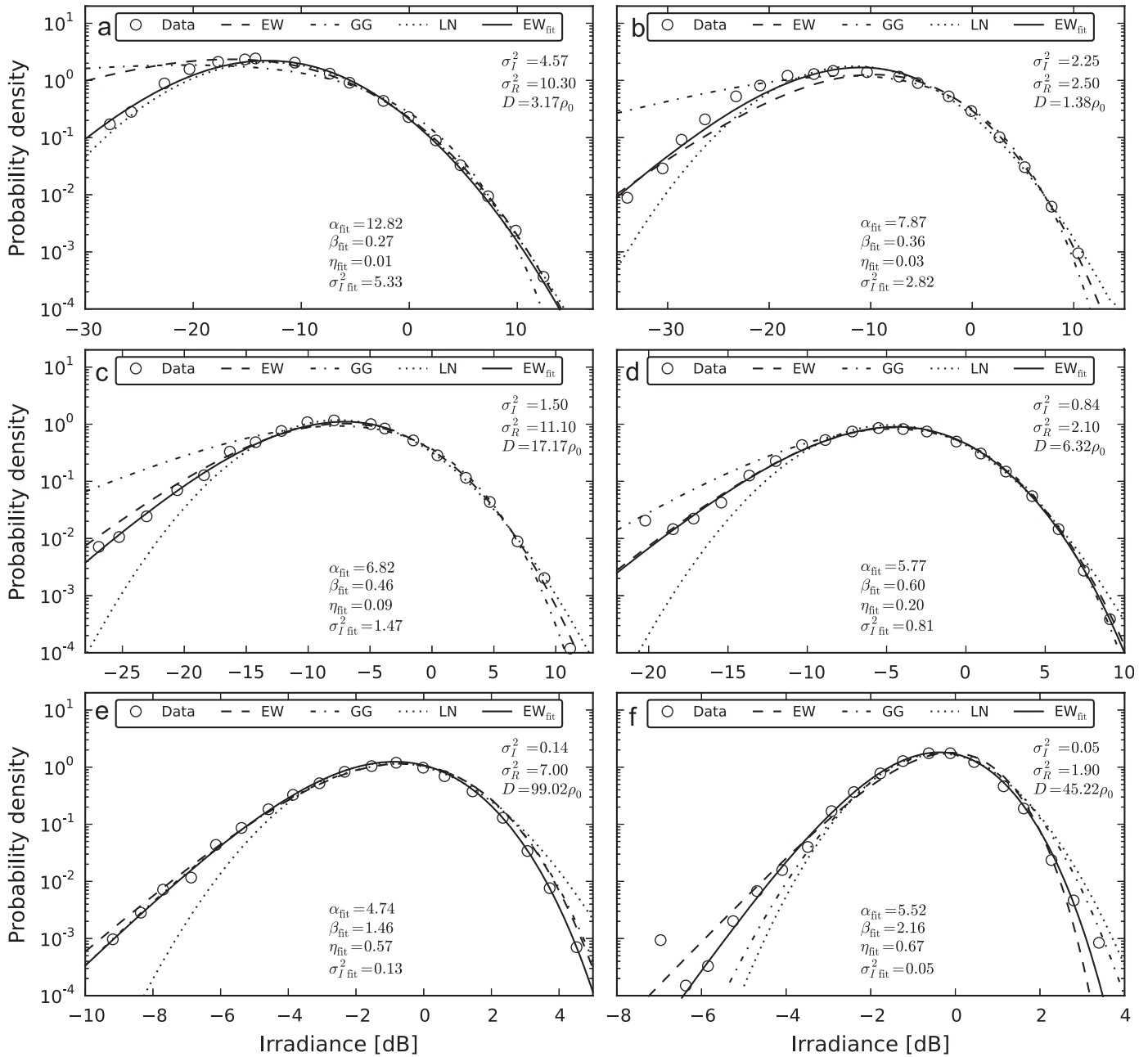


Fig. 2. Experimental data PDF from Wayne et al. [29] in comparison with the EW distribution. The curves are plotted using the parameters from Table 2. The best fit curve for the EW distribution (solid line) is shown along with its parameters values.

It has become customary in the literature to use as a decision criterion, to determine whether the LN or the GG distribution is adequate to model the irradiance PDF, the ratio between the receiving aperture diameter D and the atmospheric coherence length $\rho_0 = (1.46C_n^2 k^2 L)$. Basically, it is accepted, in the moderate-to-strong turbulence regime, that if $D \ll \rho_0$ the receiving aperture is unable to average atmospheric effects and under this condition the Gamma-Gamma distribution presents the best fit to PDF of the received irradiance data. On the contrary, if $D \gg \rho_0$ aperture averaging takes place and the PDF of the data is better described by a Lognormal distribution [6,7,36]. While, in the region of $D \sim \rho_0$ there is not a definitive answer and the best distribution to model the irradiance PDF can be either the LN or the GG distribution.

Although this is the general consensus, there are many situations where neither the LN or GG distribution can be said to

accurately model the PDF of the irradiance data in numerical simulations and experimental data, specially when aperture averaging takes place. Take for example Fig. 1(b), (e), (f), and Fig. 2(b), (c), (d) and (f). Here, it is readily seen that, although the fitting of the right tail is almost always achieved, the left tail of the PDF is the hardest section to be properly fitted by these two distributions.

However, in those situations where the LN and GG distributions both fail, the proposed exponentiated Weibull distribution presents an excellent fit to the probability density function of the irradiance data. This is particularly appreciable in the left tail of the PDF, which is of maximum importance as it defines the error-rate and fade probability. In both Figs. 1 and 2, the best fit of the exponentiated Weibull distribution to the PDF data arises as the closest fit. Note that the estimated scintillation index $\hat{\sigma}_I^2$ from the best fit EW parameters is always within a 10% of error, except

for Fig. 1e, and for Fig. 2(a) and (b) where the errors are 12.15, 16.70 and 25.15%, respectively.

It is noteworthy that the approximation given in Eq. (20) holds—within a 10% of error—when using the shape parameters α_{fit} and β_{fit} of the EW distribution estimated by the fitting algorithm, although Eq. (21) does not cope to the values of α_{fit} predicted by the fitting algorithm suggesting the need for a better approximation. It is the authors' believe that the shape parameter α for the EW distribution is somehow affected by the ratio D/ρ_0 , as previously suggested [11], and/or the Rytov variance σ_R^2 .

On the other hand, the shape of the exponentiated Weibull distribution predicted by the equations derived in Section 3.2 presents a good fit for the right-tail of the PDF data in both figures, while the prediction of left-tail shape is not robust. The closer estimation of the probability density function is achieved for the case of experimental data (see Fig. 2), where Fig. 2a is the exception and the prediction for the left-tail is very similar to that of the GG distribution. A possible explanation for this is the relative high value of the scintillation index $\sigma_I^2 = 4.57$, and that Eq. (21) is not capable of predicting values of α larger than 6. The goodness of fit of the estimated EW distribution is rather less accurate for numerical simulation data (see Fig. 1) than for the experimental data, except for Fig. 1(e) where it is a perfect fit. Once again the left-tail is the most problematic section of the PDF. Nevertheless, the predicted scintillation index $\hat{\sigma}_I^2$ from the estimated EW parameters—using Eqs. (21) and (20)—is always within less than 1% of error of the expected value (see Tables 1 and 2).

5. Conclusions

A new fading model has been presented to describe the irradiance fluctuations in FSO links, resulting in the exponentiated Weibull distribution. It has been compared with the Lognormal and Gamma–Gamma distributions, the two most widespread distributions nowadays. For the comparison previously published data have been used, including numerical simulation results and experimental data.

In every scenario the Levenberg–Marquardt least-square algorithm was used to get the best fit estimation of the EW distribution. This fit was always the closer fit to either the simulation or the experimental data, under different aperture averaging conditions and atmospheric turbulence strengths, improving the prediction made by the LN and GG distribution fits.

The expressions to estimate the shape parameters α and β of the EW distribution were given in Eqs. (21) and (20), respectively. These expressions have shown to be fairly accurate when the aperture averaging $A < 0.90$, but they have rather unpredictable behavior for values of A close to unity—i.e. for point-like apertures.

The results presented here suggest that the EW distribution presents the better fit for data under different aperture averaging conditions. Albeit, moderate-to-strong turbulence data have been used in this work, the EW suitability in weak turbulence regime has been previously demonstrated [11]. Note that, although Eq. (21) has not been tested in weak turbulence regime, the EW model validity has been assessed through the whole weak-to-strong turbulence regime by means a best fitting process using the Levenberg–Marquardt least-square algorithm. Furthermore, the exponentiated Weibull distribution have the ability to become the negative exponential distribution, when $\alpha = \beta = 1$, an attractive characteristic as it is well known that the irradiance PDF $f(I) \sim \exp(-I)$ in the limit of saturated scintillation [2,37]. For these reasons the exponentiated Weibull distribution becomes an excellent candidate to model the PDF of irradiance data under all

condition of atmospheric turbulence in the presence of aperture averaging.

Acknowledgments

This work was supported with funding from the Spanish Ministry of Science and Innovation under Contracts TEC2006-12722 and TEC2009-10025. All the code and graphics have been developed using free and open source software [38,39].

References

- [1] Beckmann P. Probability in communication engineering. Brace & World: Harcourt; 1967.
- [2] Churnside JH, Hill RJ. Probability density of irradiance scintillations for strong path-integrated refractive turbulence. Journal of the Optical Society of America A 1987;4(4):727–37.
- [3] Andrews LC, Phillips RL. *I-K* distribution as a universal propagation model of laser beams in atmospheric turbulence. Journal of the Optical Society of America A 1985;2:160–3.
- [4] Jakeman E, Pusey P. Significance of *K* distributions in scattering experiments. Physical Review Letters 1978;40:546–50.
- [5] Al-Habash MA, Andrews LC, Phillips RL. Mathematical model for the irradiance probability density function of a laser beam propagating through turbulent media. Optical Engineering 2001;40(8):1554–62.
- [6] Vetelino FS, Young C, Andrews L. Fade statistics and aperture averaging for Gaussian beam waves in moderate-to-strong turbulence. Applied Optics 2007;46(18):3780–90.
- [7] Perlot N, Fritzsche D. Aperture-averaging—theory and measurements. In: Mecherle GS, Young CY, Strykowski JS (Eds.), Free-space laser communication technologies XVI. Proceedings of the SPIE, vol. 5338; 2004. p. 233–42.
- [8] Parry G. Measurement of atmospheric turbulence induced intensity fluctuations in a laser beam. Journal of Modern Optics 1981;28(5):715–28.
- [9] Phillips RL, Andrews LC. Measured statistics of laser-light scattering in atmospheric turbulence. Journal of the Optical Society of America 1981;71(12):1440–5.
- [10] Epple B. Simplified channel model for simulation of free-space optical communications. Journal of the Optical Communications and Networking 2010;2(5):293–304.
- [11] Barrios R, Dios F. Exponentiated Weibull distribution family under aperture averaging for Gaussian beam waves. Optics Express 2012;20(12):13055–64.
- [12] Mudholkar G, Srivastava D. Exponentiated Weibull family for analyzing bathtub failure-rate data. IEEE Transactions on Reliability 1993;42(2):299–302.
- [13] Seguro JV, Lambert TW. Modern estimation of the parameters of the Weibull wind speed distribution for wind energy analysis. Journal of Wind Engineering and Industrial Aerodynamics 2000;85(1):75–84.
- [14] Fang Z, Patterson BR, Turner ME Jr. Modeling particle size distributions by the Weibull distribution function. Materials Characterization 1993;31(3):177–82.
- [15] Schleher D. Radar detection in Weibull clutter. IEEE Transactions on Aerospace and Electronic Systems 1976;12(6):736–43.
- [16] Alouini M-S, Simon M. Performance of generalized selection combining over Weibull fading channels In: Vehicular technology conference. VTC 2001 Fall. IEEE VTS 54th, vol. 3; 2001. p. 1735–9.
- [17] Lupupa M, Dlodlo M. Performance of MIMO system in Weibull fading channel—channel capacity analysis. In: EUROCON 2009, EUROCON '09. IEEE; 2009. p. 1735–40.
- [18] Churnside JH. Aperture averaging of optical scintillations in the turbulent atmosphere. Applied Optics 1991;30:1982–94.
- [19] Andrews LC, Phillips RL. Laser beam propagation through random media. second ed. Bellingham: SPIE Press; 2005.
- [20] Sagias NC, Zogas DA, Karagiannidis GK, Tombras GS. Channel capacity and second-order statistics in Weibull fading. IEEE Communications Letters 2004;8(6):377–9.
- [21] Yacoub MD. The α - μ distribution: a physical fading model for the Stacy distribution. IEEE Transactions on Vehicular Technology 2007;56(1):27–34.
- [22] Parenti RR, Sasiela RJ. Distribution models for optical scintillation due to atmospheric turbulence. Technical report. TR-1108, Lincoln Laboratory, MIT; 12 December 2005.
- [23] Abdi A, Lau WC, Alouini M-S, Kaveh M. A new simple model for land mobile satellite channels: first- and second-order statistics. IEEE Transaction on Wireless Communications 2003;2(3):519–28.
- [24] Berman GP, Bishop AR, Chernobrod BM, Nguyen DC, Gorshkov VN. Suppression of intensity fluctuations in free space high-speed optical communication based on spectral encoding of a partially coherent beam. Optics Communications 2007;208:264–70.
- [25] Jurado-Navas A, Garrido-Balsells JM, Paris JF, Puerta-Notario A. A unifying statistical model for atmospheric optical scintillation. In: Numerical simulations of physical and engineering processes, Intech; 2011. p. 181–206.
- [26] Rinne H. The Weibull distribution—a handbook. CRC Press; 2009.

- [27] Nadarajah S, Gupta AK. On the moments of the exponentiated Weibull distribution. *Communications in Statistics—Theory and Methods* 2005;34(2):253–6.
- [28] Vetelino FS, Young C, Andrews LC, Reolons J. Aperture averaging effects on the probability density of irradiance fluctuations in moderate-to-strong turbulence. *Applied Optics* 2007;46(11):2099–109.
- [29] Wayne DT, Philips RL, Andrews LC. Comparing the log-normal and gamma-gamma model to experimental probability density functions of aperture averaging data In: Majumdar C, Davis AK, (Eds.), *Free-space laser communications X*. Proceedings of the SPIE, vol. 7814; 2010. p. 78140K.
- [30] Martin JM, Flattè SM. Intensity images and statistics from numerical simulation of wave propagation in 3-D random media. *Journal of the Optical Society of America* 1998;27(11):2111–26.
- [31] Frehlich R. Simulation of laser propagation in a turbulent atmosphere. *Journal of the Optical Society of America* 2000;39(3):393–7.
- [32] Reolons J, Dios F. Accurate calculation of phase screens for the modeling of laser beam propagation through atmospheric turbulence In: Doss-Hammel SM, Kohnle A (Eds.), *Atmospheric optical modeling, measurement, and simulation*. Proceedings of the SPIE, vol. 5891; 2005. p. 51–62.
- [33] Andrews LC. Aperture-averaging factor for optical scintillations of plane and spherical waves in the atmosphere. *Journal of the Optical Society of America* 1992;9(4):597–600.
- [34] Levenberg K. A method for the solution of certain problems in least squares. *Quarterly of Applied Mathematics* 1944;2:164–8.
- [35] Marquardt D. An algorithm for least-squares estimation of nonlinear parameters. *SIAM Journal of Applied Mathematics* 1963;11:431–41.
- [36] Lyke SD, Voelz DG, Roggemann MC. Probability density of aperture-averaged irradiance fluctuations for long range free space optical communication links. *Applied Optics* 2009;48(33):6511–27.
- [37] Hill RJ, Frehlich RG, Otto WD. The probability distribution of irradiance scintillation. Technical report. ETL-270, National Oceanic and Atmospheric Administration (NOAA), Boulder, CO; January 1997.
- [38] Jones E, Oliphant T, Peterson P. *SciPy: open source scientific tools for Python*; 2001–.
- [39] Hunter JD. *Matplotlib: a 2D graphics environment* Computing Science and Engineering 2007;9(3):90–5.